■ PAPER ■

EQUIVALENT DOSE FROM SECONDARY NEUTRONS AND SCATTER PHOTONS IN ADVANCE RADIATION THERAPY TECHNIQUES WITH 15 MV PHOTON BEAMS

Isra Israngkul Na Ayuthaya[*], Sivalee Suriyapee[†], Phongpheath Pengvanich[‡]

[*]Department of Nuclear Engineering, Faculty of Engineering, Chulalongkorn University and Division of Radiology, Faculty of Radiation Oncology, King Chulalongkorn Memorial Hospital, Bangkok, Thailand

[†]Department of Radiology, Faculty of Medicine, Chulalongkorn University, Bangkok, Thailand

[‡]Department of Nuclear Engineering, Faculty of Engineering, Chulalongkorn University, Bangkok, Thailand

Received June 18, 2015 / 1st Revised August 20, 2015 / 2st Revised September 1, 2015 / Accepted for Publication September 8, 2015

The scatter photons and photoneutrons from high energy photon beams (more than 10 MV) will increase the undesired dose to the patient and the staff working in linear accelerator room. This undesired dose which is found at out-of-field area can increase the probability of secondary malignancy. The purpose of this study is to determine the equivalent dose of scatter photons and neutrons generated by 3 different treatment techniques: 3D-conformal, intensity modulated radiation therapy (IMRT) and volumetric modulated arc therapy (VMAT). The measurement was performed using two types of the optically stimulation luminescence detectors (OSL and OSLN) in the Alderson Rando phantom that was irradiated by 3 different treatment techniques following the actual prostate cancer treatment plans. The scatter photon and neutron equivalent dose were compared among the 3 treatments techniques at the surface in the out-of-field area and the critical organs. Maximum equivalent dose of scatter photons and neutrons was found when using the IMRT technique. The scatter neutrons showed average equivalent doses of 0.26, 0.63 and 0.31 mSv·Gy^{-1} at abdominal surface region which was 20 cm from isocenter for 3D, IMRT and VMAT, respectively. The scattered photons equivalent doses were 6.94, 10.17 and 6.56 mSv·Gy^{-1} for 3D, IMRT and VMAT, respectively. For the 5 organ dose measurements, the scattered neutron and photon equivalent doses in out of field from the IMRT plan were highest. The result revealed that the scatter equivalent doses for neutron and photon were higher for IMRT. So the suitable treatment techniques should be selected to benefit the patient and the treatment room staff.

Keywords : Equivalent dose, Neutron, Scatter photon, OSL

1. INTRODUCTION

Neutrons are generated by interactions of high energy photons above 10 MV with high atomic number (Z) materials. These neutrons are called photoneutrons[1]. They are produced from components of the accelerator head such as target, flattening filter, primary collimator, and secondary collimator. Interactions of high energy photons with the shielding materials around the treatment room and patient tissues can also generate photoneutrons.

External beam radiation therapy employs a high energy photon beam to cure cancer patient. Generally, 6 MV photon beam is used for the treatment. However, high energy photon beam with more than 10 MV energy is used for the treatment of deep tumors in the

Corresponding author : Isra Israngkul Na Ayuthaya, linkinpond@gmail.com
2 Banbu Siriraj Bangkoknoi, Bangkok

pelvic area such as prostate cancer. In the past decade, the intensity modulated radiation therapy (IMRT) treatment technique has gained popularity over the 3D-conformal treatment technique as the preferred treatment choice for many types of cancer. IMRT can reduce dose at the critical organ as the technique can adjust the isodose coverage to match the tumor shape. Alternative to the IMRT is the volumetric modulated arc therapy (VMAT) technique that is more recent, and many hospitals start to use it for treating certain types of cancer. It delivers dose to the whole volume rather than slice by slice while the treatment planning algorithm ensures the treatment precision to minimize dose to surrounding healthy tissue. VMAT consumes less treatment time than IMRT for the same prescribed dose.

The IMRT technique is widely used for prostate cancer treatment but it delivers higher monitor unit than the 3D-conformal technique with preserved dose. Consequently, more scatter photons and neutrons are produced inside the treatment room after employing this technique, hence increases the undesired dose to the patient and the treatment room staff. This secondary dose from scatter photons and photoneutrons can increase the risk of malignancy. Followill et al estimated the x-ray and neutron leakage from 6, 18 and 25 MV photon beams, and found the risk of secondary cancer to increase from 1.00% for 6 MV to 24.4% for 25 MV [2]. Reft et al used TLDs to measure the neutron equivalent dose at the out-of-field for the 18 MV photon beam [3]. It was found that with the IMRT technique the neutron equivalent dose normalized to the prescribed dose varied from 2 to 6 $mSv{\cdot}Gy^{-1}$. Several other studies have determined the neutron equivalent dose inside the treatment room by using Monte Carlo simulation and measurement for a variety of photon energies [4-9]. Nevertheless, no study has estimated the neutron equivalent dose for the VMAT technique. In the future, VMAT may be used to treat cancer patients more than IMRT. Thus, the neutron dose for this technique should be determined. In addition, there is no report of the dose from 15 MV photon beam for the in vivo studies of neutron dosimetry. This beam energy is utilized in many hospitals at present.

The objective of this work is to estimate the scatter photon and neutron equivalent surface dose from 15 MV photon beams for 3D, IMRT and VMAT treatments in the out-of-field and the in-field areas. The equivalent doses were measured in each critical organ using the optically stimulation luminescence (OSL) detectors. Finally, the secondary cancer risk was estimated by the organ equivalent dose (OED) concept.

2. METHODS

2.1 Treatment planning

The Eclipse treatment planning software version 11.0.31 (Varian Medical Systems, Palo Alto, CA, USA) is used to calculate the dose to 10 prostate cancer cases. The patient and plan information, age, tumor stage, planning target volume (PTV), and field size relationship are shown in Table 1. Homogeneity index (HI) = $(D_2-D_{98})/D_p$ is another homogeneity index proposed in ICRU-83, where D2 and D98 represent the doses received by 2% and 98% volumes of PTV, respectively. Conformity index (CI) is defined as ratio of volume of the body receiving the prescribed dose (Vp) to the volume of the PTV receiving the same

Table 1. Patient Characteristics, Age, Tumor Stage, PTV Volume, Field Size Relationship of 10 Prostate Cancer Cases.

ID	Age	Stage	PTV volume (cm^3)	F.S. (cm^2)
1	60	III	284	8x13
2	63	II	119	8x10
3	65	I	114	8x8
4	68	III	241	8x12
5	63	II	129	8x10
6	65	I	115	8x8
7	61	II	135	8x11
8	66	II	142	8x11
9	65	III	252	8x12
10	64	I	112	8x8

Table 2. Homogeneity Index (HI), and Conformal Index (CI) of 3D, IMRT and VMAT Treatment Techniques.

ID	HI			CI		
	3D	IMRT	VMAT	3D	IMRT	VMAT
1	1.05	1.04	1.06	1.24	1.04	1.05
2	1.06	1.04	1.06	1.12	1.05	1.02
3	1.07	1.04	1.06	1.13	1.05	1.01
4	1.05	1.03	1.06	1.14	1.05	1.04
5	1.06	1.04	1.05	1.15	1.04	1.02
6	1.06	1.05	1.06	1.12	1.05	1.03
7	1.05	1.04	1.06	1.18	1.04	1.04
8	1.06	1.04	1.05	1.20	1.04	1.02
9	1.05	1.03	1.06	1.18	1.05	1.04
10	1.07	1.04	1.06	1.13	1.04	1.02

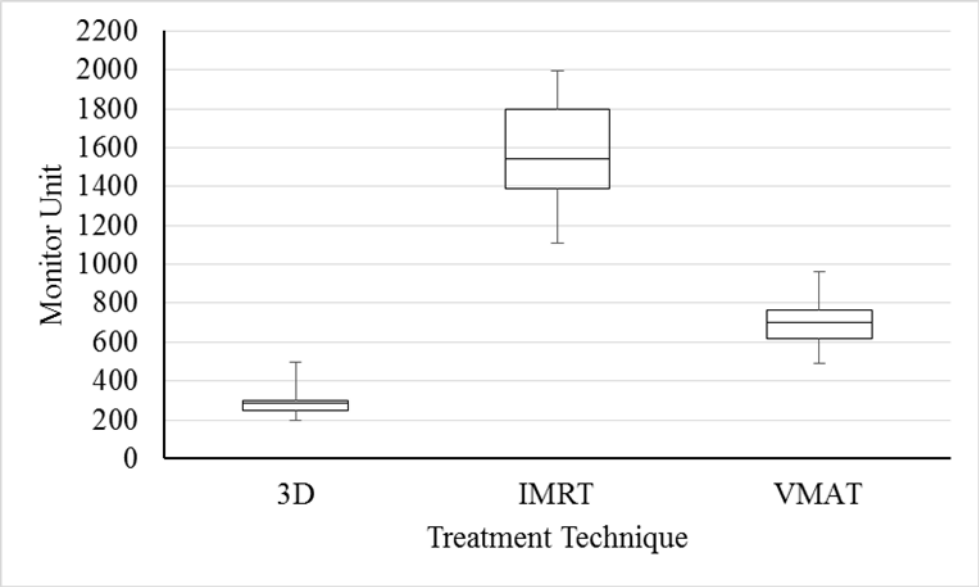

Fig. 1. The monitor units of the 3D, IMRT and VMAT treatment techniques in box plot for 10 cases.

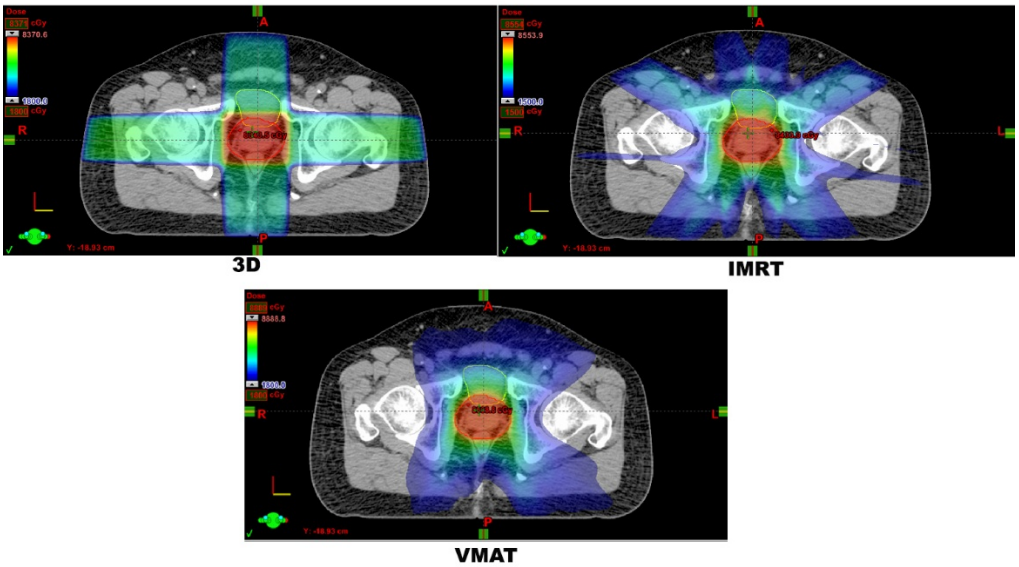

Fig. 2. Dose distribution of 3D, IMRT, and VMAT plans for prostate patient ID 2. The 3D plan used 4 fields (0, 90, 180, and 270 degree). IMRT plan used 9 fields (20, 60, 100, 140, 180, 220, 260, 300 and 340 degree). VMAT plan used 2.5 Arc (2 full arc and 1 half arc)

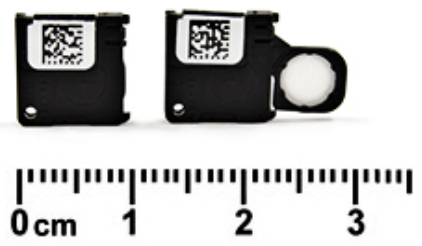

Fig. 3. The OSL nanoDot type used for radiation dosimetry.

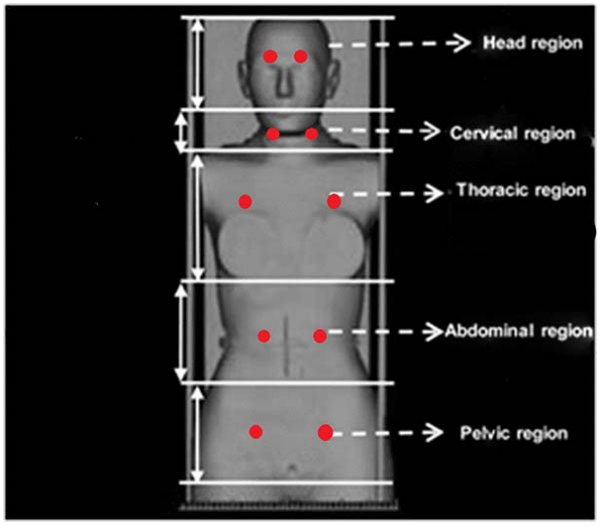

Fig. 4. The measurement of equivalent surface dose at various regions on Rando Phantom. The red dot represented the measurement position that placed on the OSL on the surface of Rando phantom.

dose (PTVp), i.e., CI = Vp/PTVp. Homogeneity index (HI), and Conformal index (CI) are shown in Table 2. Varian 23EX linear accelerator (Varian Medical Systems, Palo Alto, CA, USA) with 15 MV photon beams is used for the treatment in combination with 3 different treatment techniques. For the VMAT technique, 2.5 arcs were provided for dose calculation (2 full arcs and 1 half arc). The IMRT selected 9 fields (20, 60, 100, 140, 180, 220, 260, 300 and 340 degree) of treatment. The 3D-conformal technique employed 4 fields (0, 90, 180 and 270 degree). The prescribed dose was 2 Gy per fraction in 40 fractions for all treatment techniques. The total dose prescription is 80 Gy in all cases. Monitor unit (MU) were calculated by using the Anisotropic Analytical Algorithm (AAA) for all techniques. The monitor units of each treatment technique employed for one fraction of treatment that was shown in Fig. 1 for 10 patient cases. The dose distribution compared between each treatment technique of patient ID 2 was shown in Fig. 2. All treatment plans were delivered to the Rando phantom in the treatment room. The scatter photon and neutron equivalent doses in various areas were then measured.

2.2 Dose Measurement

The OSL detector (Inlight system, Landauer) was provided to measure the scatter photon and neutron doses. The OSL is composed of aluminum oxide (Al_2O_3:C). The OSL technology is the newest advancement in passive radiation dosimetry. The read out process uses a light emitting diode (LED) array to stimulate the detector. Then, the light emitted from the OSL detector is measured by a photomultiplier tube (PMT) counting system (Inlight system, Landauer). The type of the OSL is NanoDot that is shown in Fig. 3. The N-type (OSLN) dosimeter is capable of measuring neutron energies between 40 to 5000 keV. The OSLN contains Al_2O_3:C and is coated with $^{6}Li_2CO_3$. Neutrons interact with ^{6}Li and produce both tritium and alpha particles as shown in equation (1). These particles give up the energy in the Al_2O_3:C which in turn generates stored charge. The OSLN detectors can be annealed for reuse using the Landauer's model 50A automatic annealer. The OSL can measure the dose linearly from 10 μSv to in excess of 10 Sv. The OSL detector system was used to compare the neutron dose with Monte Carlo simulation in our previous study. The result showed the neutron doses of 5.34 and 4.53 mSv·Gy^{-1} measured by OSL and calculated by Monte Carlo at 100 cm SSD, respectively. So, OSL can use in low dose measurement.

$$ {}^{6}_{3}Li + {}^{1}_{0}n \rightarrow {}^{3}_{1}H + {}^{4}_{2}\propto \frac{Q-value}{4.78MeV} \quad (1) $$

The optically stimulation luminescence N-type (OSLN) detectors have been used for neutron dose measurement in this study. For mixed beam, the OSL measured the photon only and OSLN determined both photon and neutron. The subtraction of both reading obtained the neutron dose. Both types of the OSL were place for measurement. The OSL badge was used for dose measurement. One OSL didn't irradiate used for background control. The unscreen OSL was employed for this study. The maximum relative sensitivity of unscreen OSL varied about 3.1% of one standard deviation [10]. The OSL and OSLN were placed on the Alderson Rando phantom (RANDO®Phantoms) surface at the head, cervical, thoracic, abdominal and pelvic regions as shown in Fig. 4. The pelvis region was in

the in-field area, and the other regions were in the out-of-field area. The out-of-field region was about 20, 45, 65 and 75 cm away from the isocenter for the abdominal, thoracic, cervical, and head regions, respectively. The OSL and OSLN were put on the left and right sides of the Rando phantom for measurements. The Rando phantom was irradiated by VMAT, IMRT and 3D techniques using the actual treatment plans from 10 prostate cancer cases. The measurement was repeated 3 times, and the reading (in the unit of mSv per photon Gy) at each position was averaged. The equivalent doses were compared between the out-of- field and the in-field areas.

The scatter photon and neutron doses were measured by the OSL and OSLN in critical organs, such as brain, thyroid, lung, stomach, liver, bladder and rectum at the center of phantom slice. All organs are out-of-field of treatment area. The equivalent doses were measured in Rando phantom. The Rando phantom was scanned by CT simulation (Light Speed RT, GE). Then, the normal organs was contoured by following CT slices. The OSLs were placed in each organ of the Rando phantom by multiple positions. The equivalent doses in each organ were evaluated by averaging the dose from multiple position of OSL measurement. The Rando phantom was then irradiated by VMAT, IMRT and 3D techniques for prostate cancer. In each organ, the measurement was repeated 3 times, and its average was reported in term of mSv per photon Gy. The equivalent dose was determined in each organ. The OSL detectors have been calibrated with ^{137}Cs gamma source and OSLN detectors have been calibrated with the ^{252}Cf neutron source because the energy range of ^{252}Cf covers the energy range of the photoneutrons generated inside the treatment head of the linear accelerator based on the Monte Carlo simulation result. The neutron spectrum was simulated for the 15 MV photon beam modeled after the Varian 23EX linear accelerator. The number of initial electrons used for the simulation was 10 millions. The components of Linear accelerator head were created according to the data from manufacturer. However, a smaller boundary is used instead of the actual room geometry to reduce the calculation time. The neutron spectra were calculated by the MCNP5 code at the target, collimator jaws, and isocenter of the field, as shown in Fig. 5. The average energy is about 0.25 MeV. The neutron spectrum energy was employed to calculate the neutron dose correction (NCF). The neutron dose was calculated by using the radiation weighting factor recommendations of ICRP 103 [11].

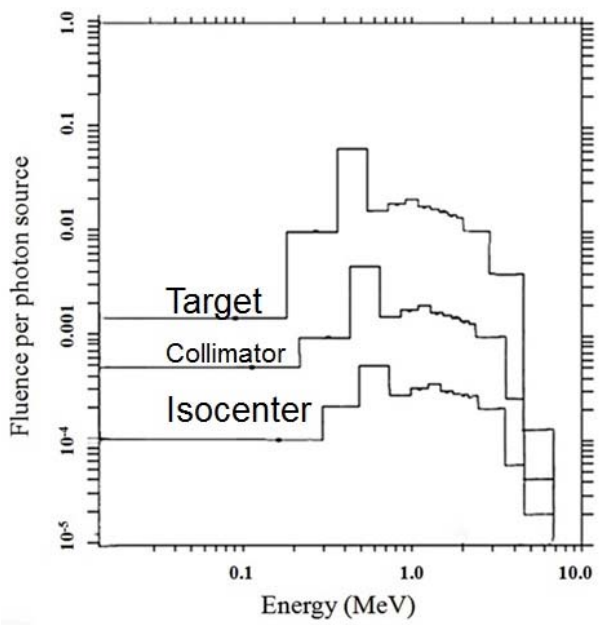

Fig. 5. Neutron spectra simulated by Monte Carlo Method at the target, the primary collimator and the isocenter positions. The average energy is 0.25 MeV for each component.

2.3 Secondary cancer risk estimation

In radiotherapy during the past decades has made the risk of developing a radiation-induced secondary cancer as a result of dose to normal tissue a highly rel evant survivorship issue. The secondary cancer incidence rates after RT and calculations of secondary cancer incidence rates for comparing RT techniques have been based on the evaluation of the OED. The model parameters used in this work were obtained the information from Japanese atomic bomb and patient of medical radiation treatment. Cancer risk is only proportional to average organ dose as long as the dose–response curve is linear. At high dose it could be that the dose–response relationship is nonlinear.

Three different dose–response relationships are considered here [12, 13]. The first is a linear response over the whole dose range:

$$OED = \frac{1}{V}\Sigma_i V_i D_i \tag{2}$$

The second is a linear-exponential dose–response relationship of the form:

$$OED = \frac{1}{V}\sum_i V_i D_i e^{(-\propto D_i)} \quad (3)$$

and the third is a dose–response, which is flattening at high dose, a so-called plateau dose–response described by:

$$OED = \sum_i V_i \frac{(1-e^{(-\delta D_i)})}{\delta} \quad (4)$$

In a radiotherapy, patient respect to radiation-induced cancer. Unfortunately, the shape of the underlying dose–response relationship for radiation-induced cancer is not very well known for doses larger than 2 Gy. However, it can be confidently expected that the real dose–response lies between the extremes of a linear. Therefore, this study estimates secondary cancer risk by taking both possibilities into account. In addition, we use a plateau dose–response curve, which is located approximately in the middle of the two extreme curves. The OED of brain, thyroid, lung, stomach and liver (out of field organs) is estimated for 3D, IMRT, and VMAT treatment technique.

3. RESULTS AND DISCUSSION

3.1 Equivalent surface doses within the in-filed and out-of-field regions.

The average scatter photon and neutron equivalent doses at the head, neck, chest, abdomen regions from 10 prostate cancer treatment cases via the 3D, IMRT and VMAT techniques are shown in Table 3. The neutron equivalent dose decreased in the out-of-field region when the regions was far from the isocenter. In the head region, the neutron equivalent dose was less than in the abdomen region about 2 times. The distance between the two positions was 55 cm. The neutron dose decreased at further distance. Zabihzadeh et al reported the neutron equivalent dose of 4.1 mSv·Gy^{-1} at isocenter and 0.79 mSv·Gy^{-1} at a distance of 100 cm out-of-field in air for 40x40 cm^2 field in 15 MV photon beam based on the calculation by Monte Carlo simulation [14]. In all cases, the neutron doses from the IMRT plan were higher than from the VMAT and the 3D conformal plans. The neutron doses from VMAT plan were slightly higher than the dose from the 3D plan in all regions. The neutron dose depended on the MU which was highest in the case of IMRT for a same prescribed dose in treatment plan. Therefore, the suitable treatment technique can helps for reducing neutron dose to out-of-field of patient.

For the scatter photon equivalent doses, the photon dose per Gy also decreased further away from the isocenter. The scatter photon dose was highest in the case of 3D plan in abdomen region. This was because the measurement point was near the isocenter that generated the scatter photon from primary beam. The scatter photon doses from IMRT were found to be highest in the out-of-field regions. They were 0.26, 0.63, and 0.31 mSv·Gy^{-1} at abdomen surface region which was 20 cm from isocenter for 3D, IMRT and VMAT, respectively. The scatter photon dose depended on the beam irradiated time. The IMRT plan consumed the highest MU per one treatment fraction. The scatter photon dose decreased further away from the isocenter. In out-of-field, the scatter photon equivalent doses were at least 10 times higher than the neutron equivalent dose.

Limitation of this study, the neutron dose measured on the surface of phantom should be used the OSL detector placing on multiple locations in a transverse plane. It can prove the effect of the beam direction in IMRT and VMAT plan and can evaluate the neutron dose more information. This study can measure dose only anterior direction because a number of OSL detectors are not enough for multiple position measurements. Many OSL detectors were used for organ dose measurement inside the phantom and surface dose on

Table 3. The Average Scatter Photon and Neutron Equivalent Surface Doses Measured on Head, Cervical, Thoracic, Abdominal, and Pelvic Regions for 3 Treatment Techniques in the Unit of mSv·Gy^{-1} for 10 Prostate Cancer Treatment Cases.

Region	3D (mSv·Gy^{-1})		IMRT (mSv·Gy^{-1}))		VMAT (mSv·Gy^{-1})	
	Photon	Neutron	Photon	Neutron	Photon	Neutron
Head	1.71±0.15	0.12±0.12	1.92±0.14	0.21±0.11	1.87±0.16	0.16±0.11
Cervical	1.62±0.17	0.13±0.13	2.65±0.18	0.24±0.15	2.07±0.17	0.18±0.12
Thoracic	4.85±0.24	0.21±0.16	6.36±0.26	0.51±0.17	3.78±0.12	0.28±0.15
Abdominal	6.94±0.28	0.26±0.18	10.17±0.33	0.63±0.20	6.56±0.28	0.31±0.19

Table 4. The Average Scatter Photon and Neutron Equivalent Doses Measured in 7 Organs for 3 Treatment Techniques in the Unit of mSv·Gy^{-1} for 10 Prostate Cancer Treatment Cases.

Region	3D (mSv·Gy^{-1})		IMRT (mSv·Gy^{-1}))		VMAT (mSv·Gy^{-1})	
	Photon	Neutron	Photon	Neutron	Photon	Neutron
Brain	1.65±0.15	0.10±0.10	3.91±0.14	0.20±0.11	1.86±0.15	0.16±0.10
Thyroid	1.87±0.16	0.13±0.12	4.44±0.18	0.28±0.13	2.01±0.17	0.22±0.12
Lung	2.11±0.18	0.28±0.12	6.52±0.18	0.41±0.14	2.76±0.18	0.39±0.15
Stomach	2.58±0.21	0.52±0.14	9.35±0.22	0.69±0.17	3.53±0.21	0.52±0.18
Liver	2.79±0.21	0.56±0.16	10.23±0.23	0.73±0.17	3.78±0.22	0.57±0.18

the phantom in the same time. In the future work, the neutron equivalent dose should be measured by other detectors. The neutrons are very difficult for measurement because it varies the energy range. In each energy of neutron is suitable with different detectors for measurement.

3.2 Equivalent doses in the organs.

The average scatter photon and neutron equivalent doses in 7 organs based on 3 treatment techniques are shown in Table 4. In all cases, the neutron doses from the IMRT plan were highest. Brain, which was the furthest distance from the isocenter, received less scatter photon and neutron doses than other organs. Scatter photon doses from the IMRT plan were also observed to be higher than from the other techniques in all organs. The neutron equivalent dose decreased 2-3 times in out-of-field organs when the organ was further from the isocenter. Kry et al have also estimated the out-of-field photon and neutron equivalent dose from step and shoot IMRT technique, as well as the neutron equivalent dose to each critical organ and the risk of malignancies. Neutrons equivalent dose range was 2.5-9.0 μSv per MU in each organ when photon treatment energies were 15 MV for IMRT technique [15]. The value agreed well with our study. The equivalent doses from scatter photons were higher than from neutrons in all organs and treatment techniques. The equivalent doses of neutron were 10% of scatter photon, but in several organs they could be as high as 20%.

3.3 Secondary cancer risk estimation

The secondary cancer risk was estimated in term of ODE. The ODE was calculated for brain, thyroid, lung, stomach, and liver normalized to IMRT treatment technique. Fig. 6 shows relative risk of prostate cancer patient at out of field region in each treatment

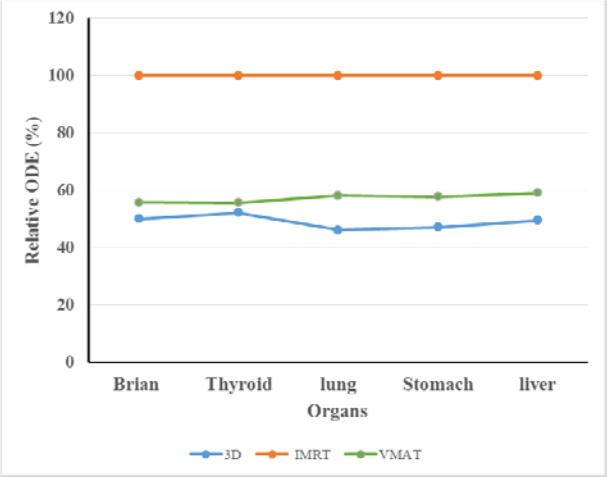

Fig. 6. The relative OED of each organ to normalize to VMAT plan for 3D, IMRT and VMAT plan. The secondary cancer risk of each organ of 3D and VMAT is less than IMRT.

technique. Secondary cancer risk of all out of field organs decreased in the 3D and VMAT plans when compared with IMRT plan. The risk decreased about 2 times because effect of scatter and leakage of IMRT plan was more than 3D and VMAT plans. IMRT plan spend more MU per fraction. Although the 3D plan is the least probability of cancer risk, for clinical, VMAT plan is a good choice for treatment the prostate cancer because it can reduce the secondary cancer risk but it can provide the dose distribution to conform to tumor and spare normal organ like a IMRT plan.

4. CONCLUSIONS

The scatter photon and neutron equivalent surface doses decreased further away from the isocenter. The neutron dose should be concerned when patients are treated by photon energy of more than 10 MV because it can significantly generate photoneutrons inside the treatment room. The scatter photon and neutron equiv-

alent doses vary in different treatment techniques. IMRT technique, which consumes the highest MU per treatment fraction for the same prescribed dose, can generate the higher neutron dose than other treatment techniques. Although the neutron dose from the VMAT technique is slightly higher than from the 3D technique, it is overall a better choice for treatment because it can decrease the neutron dose to patient while keeping the isodose coverage and sparing normal organ the same as the IMRT technique. The equivalent dose of out-of-field organs receives wide range of neutron doses, and in some cases the doses can be as high as 20% of the doses from scatter photons. These can pose additional risk of secondary malignancy to patient. The treatment energy of photon beam should be selected to be less than 10 MV if possible in order to reduce the unwanted dose and the risk of secondary malignancy to the patients and the treatment room staff. The suitable of treatment plan can help to decrease the risk of secondary cancer to patient in the future.

ACKNOWLEDGEMENTS

The authors would like to thanks the medical physicist team at the Division of Radiation Oncology, King Chulalongkorn Memorial Hospital for their assistance with data collection. We would like to thanks staff of Division of Radiation and Medical Devices, Department of Medical Science, Ministry of Public Health for OSL detector and measurement. We would like to thanks The 90th Anniversary of Chulalongkorn University Fund (Ratchadapiseksompot Endowment Fund) supports the fund for this study.

REFERENCES

1. Chibani O, Ma CC. Photonuclear dose calculations for high-energy photon beams from Siemens and Varian linacs. Med Phys. 2003;30:1990-2000.
2. Followill D, Gies P, Boyer A. Estimates of whole-body equivalent produced by beam intensity modulated conformal therapy. Int J Radiat Oncol Bio Phys. 1997; 38(3):667-672.
3. Reft CS, Runkel-Muller R, Myrianthopoulos L. In vivo and phantom measurements of the secondary photon and neutron doses for prostate patients undergoing 18 MV IMRT. Med Phys. 2006;33(10): 3734-3742.
4. Howell RM, Kry SF, Burgett E, et al. Secondary neutron spectra from modern Varian, Siemens, and Elektalinacs with multileaf collimators. Med Phys. 2009;36(9):4027-4038.
5. Nedaie HA, Darestani H, Banaee N, et al. Neutron dose measurements of Varian and Elektalinacs by TLD600 and TLD700 dosimeters and comparison with MCNP calculations. Med Phys. 2014;39(1): 10-17.
6. Passmore C, Kirr M. Neutron response characterization of an OSL neutron dosimeter. Radiat Prot Dosim. 2011;144:155-160.
7. Martinez-Ovalle SA, Rarquero R, Gomez-Ros JM, et al. Ambient neutron equivalent dose outside concrete vault rooms for 15 and 18 MV radiotherapy accelerators. Radiat Prot Dosim. 2012;148 (4):457-464.
8. Bednarz B, Xu XG. Monte carlo modeling of a 6 and 18 MV Varian Clinac medical accelerator for in-field and out-of-field dose calculations: development and validation. Phys Med Biol. 2009;54(4): 43-57.
9. Meo XS, Kase KR, Liu LC, et al. Neutron sources in the Varian Clinac 2100C/2300C medical accelerator calculated by the EGS4 code. Health Phys. 1997;72:524-530.
10. Cygler JE, Yukihara E. Optically Stimulated Luminescence (OSL) dosimetry in radiotherapy. AAPM 51th annual meeting, California. 2009.
11. ICRP (2007), The 2007 recommendation of ICRP. Annals of the ICRP, ICRP Publication 103.
12. Schneider U, Walsh L. Cancer risk estimates from the combined Japanese A-bomb and Hodgkin cohorts for doses relevant to radiotherapy. Radiat Environ Biophys. 2008;47:253–263.
13. Yoon M, Ahn SH, Kim J, et al. Radiation-induced cancers from modern radiotherapy techniques: intensity-modulated radiotherapy versus proton therapy. Int J Radiat Oncol Biol Phys. 2010;77(5): 1477-1485.
14. Kry SF, Salehpour M, Followill D, et al. Out-of-field photon and neutron equivalent doses from step-and-shoot intensity-modulated radiation therapy. Int J Radiat Oncol Bio Phys. 2005;62(4):1204-1216.
15. Zabihzadeh M, Ay MR, Allahverdi M, et al. Monte Carlo estimation of photoneutrons contamination from high-energy x-ray medical accelerators in treatment room and maze: a simplified model. Radiat Prot Dosim. 2009;135(1):21-32.